ROYAL SOCIETY OF CHEMISTRY

Journal Name

ARTICLE

Linear Dendronized Polyols as a Multifunctional Platform for a Versatile and Efficient Fluorophore Design

Received 00th January 20xx, Accepted 00th January 20xx

DOI: 10.1039/x0xx00000x

www.rsc.org/

Ying Li,^{‡,a} Katharina Huth,^{‡,b} Edzna S. Garcia,^a Benjamin J. Pedretti,^a Yugang Bai,^a Gretchen A. Vincil,^a Rainer Haag^b and Steven C. Zimmerman*,^a

Fluorescent linear dendronized polyols (LDPs) were prepared in two steps involving a ring-opening metathesis polymerization (ROMP) followed by acid-catalyzed deprotection. The resulting water-soluble fluorophores are compact in size (< 6 nm) and show similar photostability compared to previously reported crosslinked dendronized polyols (CDPs) and significantly improved photostability compared to the free fluorophores. In contrast to the synthesis of CDPs, the production of LDPs requires less preparation time, synthetic effort, and significantly less Grubbs catalyst. The photophysical properties, including the photostability and emission wavelength of LDPs, can be further fine-tuned by incorporating different combinations of dendronized monomers and fluorophores. Interestingly, fluorescence resonance energy transfer (FRET) was observed when two different kinds of fluorophores were incorporated into the LDPs. This provides a new type of fluorophore with a large Stokes shift allowing fluorescence detection with reduced background overlap. Cytotoxicity and fluorescence imaging studies confirmed the biocompatibility of these LDPs, which render them as potential candidates for biological applications.

Introduction

Fluorophores are used widely in fluorescence imaging to visualize the location of biomolecules, track biological processes, quantify the strength of intermolecular interactions, and to detect small molecules and metal ions.¹⁻¹⁷ To allow efficient labeling and accurate tracking in fluorescence microscopy, it is crucial to use fluorophores that are cell permeable and that have high brightness and prolonged stability.2 However, it is challenging to achieve all of these features simultaneously. Some commonly used fluorescent organic dyes possess a low molar absorption coefficient or a low quantum yield in water, and many have a high propensity for photobleaching.³⁻¹¹ Inorganic nanoparticles, including quantum dots, can serve as highly stable fluorescent bioprobes;12-17 however, to become biocompatible they require coatings that can increase their size significantly.18 In addition to toxicity concerns that arise with many of the metals used, this large size can make it either difficult for the nanoparticle to enter the cell or may alter the localization and behavior of the biomolecule of interest. 19-20

Polymer nanoparticles with covalently attached organic dyes provide an attractive alternative approach to develop the next-generation fluorophores for bioimaging.^{6,21-24} The polymer can solubilize poorly soluble dyes in water and protect them from photobleaching and self-quenching by inhibiting self-association. We recently introduced fluorescent organic nanoparticles (ONPs),

which achieved high brightness and photostability by the incorporation of multiple fluorescein units into a polymer backbone.²⁵ However, to render the ONPs water-soluble a dihydroxylation process using potassium osmate was required, limiting the dyes that could be used and making the synthetic route less desirable due to the toxicity of osmium.

The use of osmium was avoided by employing crosslinked dendronized polyol (CPDs) as a general, compact, and globular platform to achieve brighter and more stable fluorophores.²⁶ The multiple fluorescent units incorporated along the single polymer chain are stabilized by the polymer backbone, resulting in significantly brighter molecules. Multiple hydroxyl groups on the polyglycerol (PG) dendrons endowed the CDPs with intrinsic watersolubility. Despite this benefit, the polymer preparation process for CDPs takes up to a week. Furthermore, the preparation included a ring-closing metathesis (RCM) step that required a large excess of Grubbs catalyst, which, in turn, led to trace amounts of residual ruthenium that was difficult to remove from the final fluorescent polymeric nanoparticles. Here we report a simplified synthetic strategy for dendronized polymer nanoparticles that affords similar photostability without the dihydroxylation or RCM steps. Additionally, this versatile synthetic approach to LDPs²⁷⁻³³ allows for a facile incorporation of other moieties into the polymer platform, including multi-sulfide-containing dendrons, dendronized fluorophores, and two different kinds of fluorophores allowing for fluorescence resonance energy transfer (FRET) pairs.

Results and discussion

Polymer synthesis

To shorten the preparation process for dendronized polymer nanoparticles and reduce the amount of ruthenium catalyst

^{a.} Department of Chemistry, University of Illinois at Urbana-Champaign, Urbana, 505 S Mathews Ave, Illinois 61801, USA. E-mail: sczimmer@illinois.edu

^{b.} Institute of Chemistry and Biochemistry - Organic Chemistry, Freie Universität Berlin, Takustr. 3, 14195 Berlin, Germany.

[‡] These authors contribute equally.

[†] Electronic Supplementary Information (ESI) available: experimental details, including synthesis, photophysical characterization, and biological studies of the polymers. See DOI: 10.1039/x0xx00000x

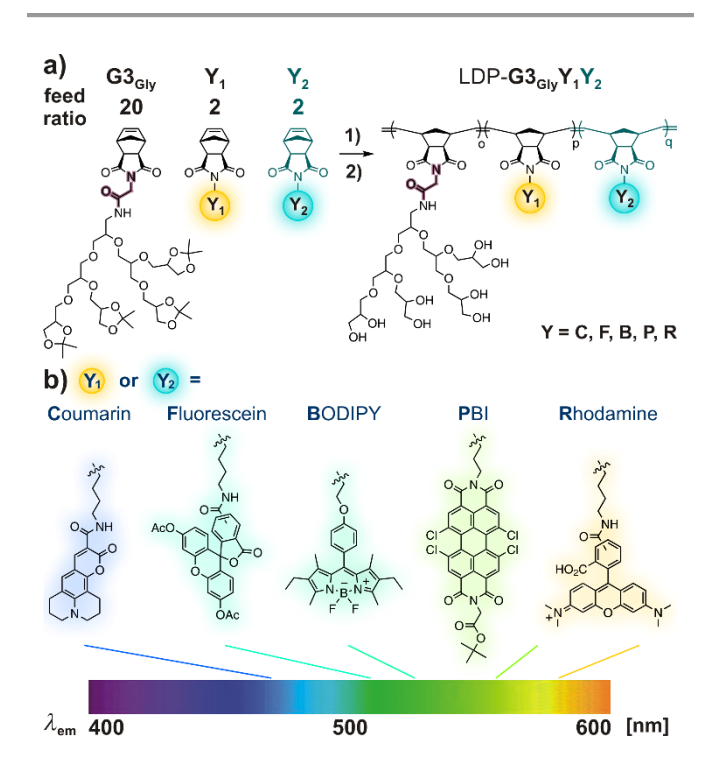
ARTICLE Journal Name

Table 1. Photophysical properties of free fluorophores, CDPs, and LDPs at a concentration of 1.5 μ M for absorption and 0.15 μ M for emission measurements in 0.1 M phosphate buffer (PB, pH 7.4) at 20 °C.

	Free fluorophore ²⁶			CDP- G3 _{Gly} Y ²⁶			LDP- G3 _{Gly} Y		
Fluorophore Y	ϵ^a	\mathcal{O}_{f^b}	B ^c	ϵ^a	\mathcal{O}_{f^b}	B ^c	ϵ^a	\mathcal{O}_{f}^{b}	B ^c
	(M ⁻¹ cm ⁻¹)	(%)	(M ⁻¹ cm ⁻¹)	(M ⁻¹ cm ⁻¹)	(%)	(M ⁻¹ cm ⁻¹)	(M ⁻¹ cm ⁻¹)	(%)	(M ⁻¹ cm ⁻¹)
Coumarin	10 300	96	9.9	38 300	34	13	55 800	40	22
Fluorescein	74 700	95	71	157 800	71	112	159 00	51	81
$BODIPY^d$	4 300	1.3	0.056	47 800	46	22	113 000	53	60
$\mathbf{P}BI^d$	29 400	3.3	0.97	78 300	4.6	3.6	93 400	4	3.7
Rhodamine	91 700	12	11	181 800	11	20	140 000	9	13

 $^{^{}o}$ Molar absorption coefficient ε , Equation S1, ESI † . b Fluorescence quantum yield Φ_{f} , Equation S2, ESI † . c Brightness B, Equation S3, ESI † . d Water-insoluble fluorophores (BODIPY and PBI) were first dissolved in dioxane and then diluted with 0.1 M PB.

needed, we investigated a streamlined approach for the polymer synthesis. The crosslinking RCM step that was necessary to generate the previously reported CDPs was eliminated to afford short-chain, low molecular weight polymers. We probed the protective effect of these novel uncrosslinked linear dendronized polyols (LDPs) (Scheme 1a) on a set of five different fluorophores that cover a 150 nm range in the visible light region. Two kinds of norbornene monomers were used in the synthesis of each LDP (see monomer synthesis, ESI+). The first is glycine-modified 3rd-generation PG dendron monomer²⁶ G3_{Gly} (Scheme 1a) and the second is one of five fluorophore-containing monomers $^{25-26}$ Y where Y = Coumarin, Fluorescein, BODIPY, Perylene bisimide (PBI), or Rhodamine, which are hereinafter abbreviated by the first letter of their name (Scheme 1b). Linear random copolymers were synthesized by ringopening metathesis polymerization (ROMP) using monomers G3_{Gly}, \mathbf{Y} , and 3^{rd} -generation Grubbs catalyst with a molar ratio of 20 : 2 : 1.



Scheme 1. a) Synthesis and feed ratios of linear dendronized polyols LDPs- $G3_{Gly}Y_1Y_2$ with glycine-linked dendron monomer $G3_{Gly}$ and one or two fluorophore monomers Y. The second fluorophore Y_2 shown in dark green is optional and was exclusively introduced for the FRET study. The Gly-linker is shaded in purple. 1) 3^{rd} -generation Grubbs catalyst, DCM, RT, 15 min and 2) TFA, DCM, RT, 1 h. b) Structures of fluorophore monomers Y with Y = Coumarin, Fluorescein, BODIPY, PBI, or Rhodamine.

Subsequent deprotection of the acetal-protected diols with trifluoroacetic acid (TFA) afforded water-soluble, fluorescent, dendronized polymers LDPs- $\mathbf{G3}_{Gly}\mathbf{Y}$ (see polymer synthesis, ESI†). To tune the optical properties of the LDPs, the polyols were also prepared with two different fluorophores resulting in LDPs- $\mathbf{G3}_{Gly}\mathbf{Y_1Y_2}$, which were used for the FRET study. Minimizing the synthetic effort, LDPs can be prepared in two steps in a single day whereas the preparation of CDPs required four steps extending the preparation time to completion to about one week.

The LDPs were characterized by ¹H NMR spectroscopy, dynamic light scattering (DLS), and gel permeation chromatography (GPC, see polymer characterization, ESI†). A 5.53 nm hydrodynamic diameter was determined for representative LDP-**G3**_{GIV}**F** by DLS (Figure S7, ESI†) with a similar size expected for the other LDPs reported, whose fluorophores prevented DLS analysis. Some of the fluorophore-containing LDPs equipped with one fluorophore feature narrow polydispersity indices (PDIs) between 1.0 and 1.51 as determined by GPC (see Table S1, ESI†). Representative LDP-**G3**_{GIV}**F** gave a molecular weight of 22 kDa determined by GPC, which is smaller compared to the CDP-**G3**_{GIV}**F** analogue (79 kDa).

Photophysical properties and photostability study

We hypothesized that the multiple hydroxyl groups on LDPs of low molecular weight would be sufficient to impart the attached fluorophores with photostability and water solubility. To test this idea, the photophysical properties and photostability of LDPs were studied in phosphate buffered (PB) solutions (0.1 M, pH 7.4) and compared to the free fluorophores and previously reported CDPs. As shown in Table 1, LDPs have comparable molar absorption coefficients, fluorescence quantum yields (FQYs), and brightness values to the previous CDPs (Figure S10a, ESI†). All LDPs, except for LDP-**G3**_{GIV}**R**, exhibited improved molar absorption coefficients with the greatest improvement observed for BODIPY. Compared to CDPs, LDPs containing coumarin and BODIPY showed an increase in FQY and brightness. Fluorescein, on the other hand, showed a decrease in FQY and brightness in the CDP scaffold. This may be due to fluorescein being more sensitive to its environment compared to the other dyes.34-37

To investigate the photostability, PB solutions of LDPs were irradiated with blue light at 470 nm from an LED while the fluorescence intensity was measured over a period of 4 h (see Figure 1 and details in ESI†). The photostability of coumarin, fluorescein, and rhodamine were similar in both LDPs and CDPs. The photostability of PBI was improved by a factor 1.75 with the LDP scaffold compared to CDPs. Among all the dyes tested, PBI has the largest conjugated system that might non-covalently interact with residual ruthenium catalyst byproducts, possibly leading to a

Journal Name ARTICLE

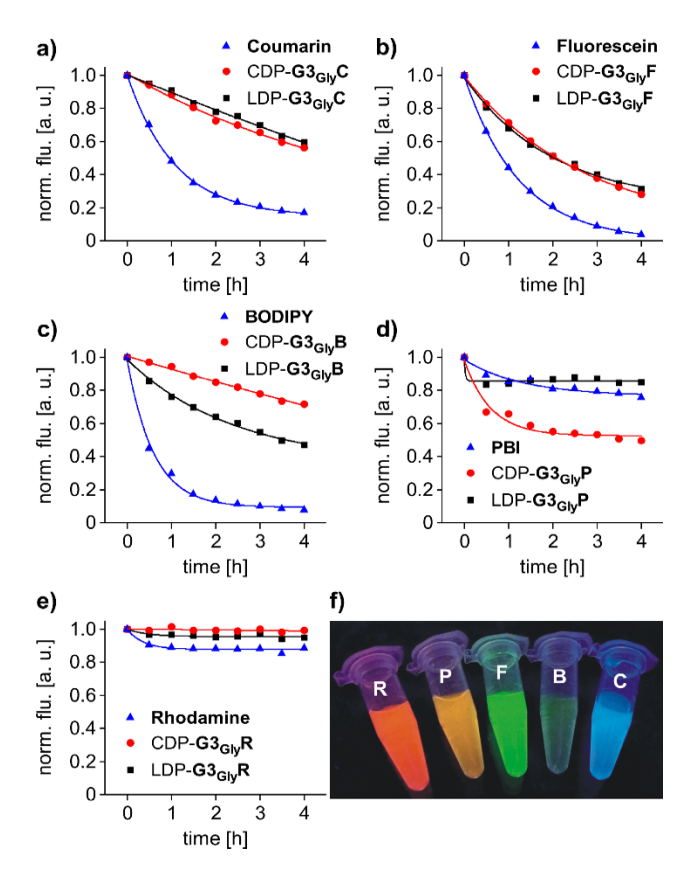


Figure 1. a) - e) Normalized fluorescence intensities over time during the photostability study with free fluorophores, CDPs, and LDPs. PB solutions (0.1 M, pH 7.4) of the corresponding compounds (0.15 μ M) were irradiated with blue light at 470 nm over 4 h while the fluorescence intensities were measured (for spectra of absolute fluorescence intensities see Figure S11, ESI†). f) Picture of LDPs in PB solution at a concentration of 25 μ M, illuminated with a UV lamp at 365 nm.

lower photostability in CDPs. In the case of BODIPY, LDP-**G3**_{GIV}**B** was less stable compared to CDP-**G3**_{GIV}**B** but remained 2000 times brighter than free BODIPY after 4 h of irradiation (see Figure S11 c, ESI+). The lower protection afforded in the LDP most likely arises because the short polymer chains of LDPs cannot afford sufficient shielding to protect the complex structure of BODIPY from bleaching. Overall, these results confirm that the RCM-mediated crosslinking step was not necessary to afford stable and bright fluorophores as shown by the comparable optical properties and similar photostability of the fluorophores within the CDP and LDP scaffolds. Once we ensured that the Gly-linked CDPs and LDPs provide similar photostability, we focused on simplifying the monomer synthesis, which led us to the Cys-linked LDPs.

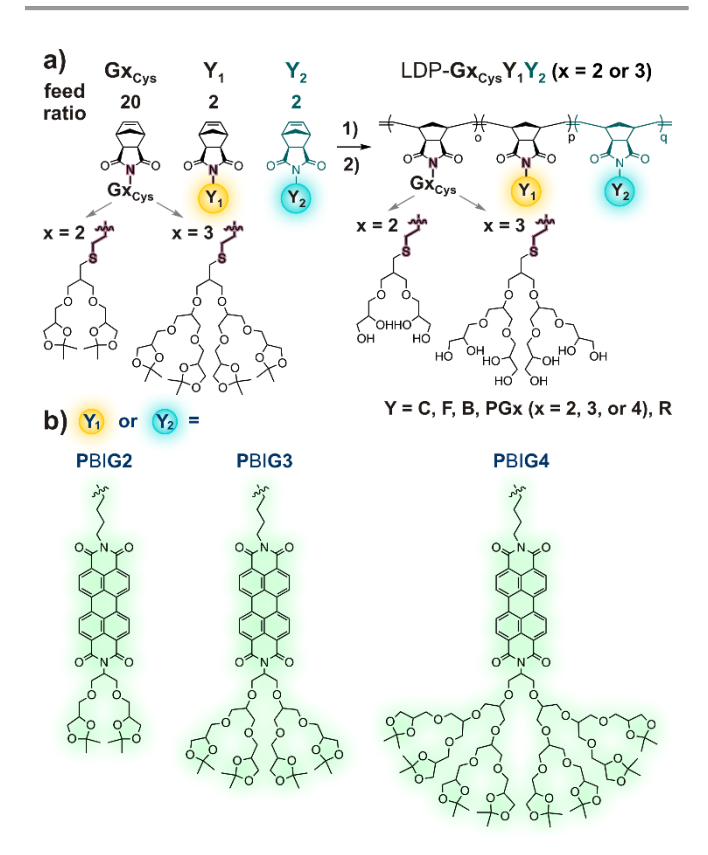
Dendronized monomer synthesis

In addition to streamlining the polymer synthesis, we investigated a simplified approach to prepare dendronized monomers. The synthesis of dendronized monomer $\mathbf{G3_{Gly}}$ required 11 steps starting from commercially available materials with an overall yield of 13%.²⁶ The synthesis of the new dendronized monomer $\mathbf{G3_{Cys}}$ takes only 4 steps with an overall yield of 33% (Scheme 2 and S3). The time-saving approach in the new synthesis uses a thiol-ene reaction between cysteamine and alkene $\mathbf{G3_{Cys}}$ -ene²⁰ to afford amine-cored 3rd-generation dendron $\mathbf{G3_{Cys}}$ -NH₂ in a total of 3 steps starting from triglycerol. The fourth step involves a condensation of norbornene anhydride with $\mathbf{G3_{Cys}}$ -NH₂ to yield the final dendronized monomer $\mathbf{G3_{Cys}}$ (see Scheme S3, ESI†). The resulting cysteamine-containing

 3^{rd} -generation PG dendron monomer $G3_{Cys}$ was used to replace $G3_{Gly}$ in the following reported LDPs to further demonstrate the modularity of our polymer system. Additionally, 2^{nd} -generation cysteamine dendron monomer $G2_{Cys}$ was prepared following the alternative and improved synthetic approach (see Scheme S2, ESI†). As a result, the streamlined synthesis of the dendron monomer and the linear polymer approach significantly improve the entire polymer preparation process. Besides the glycine-linked LDPs- $G3_{Gly}Y$, a series of cysteine-linked LDPs- $Gx_{Cys}Y$ (x=2 or 3) was prepared with either cysteine-modified dendron monomer $G2_{Cys}$ or $G3_{Cys}$ and one or two fluorophore monomers Y where Y=C oumarin, Fluorescein, BODIPY, dendronized PBIGx, or Rhodamine as shown in Scheme 2a. In the cysteine-linked LDPs, the previously used PBI was replaced by dendronized PBIGx (x=2, 3, or 4) to investigate the effect of enhanced dendronization (Scheme 2b).

Advanced dendron monomer

Fluorescein is known to have low photostability, in part because it is prone to oxidation upon irradiation. The photostability of fluorescein was not significantly improved with either the CDP or LDP architecture (around 13% improvement, see Figure S11 and Table S3, ESI†). Benefiting from the modularity of LDPs, we sought to enhance the protective effect of the macromolecular scaffold to further improve the photostability of fluorescein. Anti-fading agents such as n-propylgallate and Trolox are commonly added to the



Scheme 2. a) Streamlined synthesis and feed ratios of linear dendronized polyols LDPs- $Gx_{Cys}Y_1Y_2$ (x=2 or 3) with new cysteine-linked dendron monomers $G2_{Cys}$ or $G3_{Cys}$ and one or two fluorophore monomers Y. The second fluorophore Y_2 shown in dark green is optional and was exclusively introduced for the FRET study. The Cys-linker is shaded in purple. 1) Grubbs catalyst 3^{rd} -generation, DCM, RT, 15 min and 2) TFA, DCM, RT, 1 h. For structures of the fluorophore monomers Y with Y = Coumarin, Fluorescein, BODIPY, and Rhodamine see Scheme 1b. b) Structures of the new dendronized fluorophore monomers Y BIGX (X = X, X = X = X in three different dendron generations.

ARTICLE Journal Name

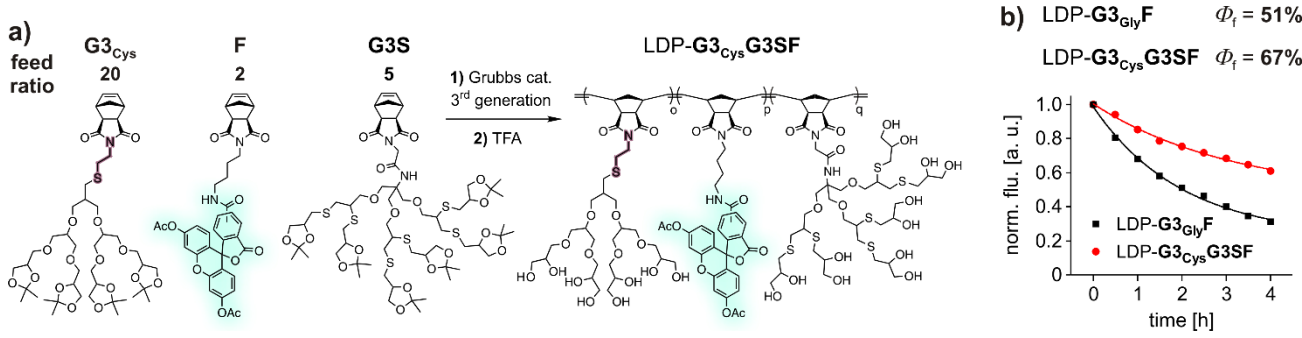


Figure 2. a) Synthesis and feed ratios of multi-thioether-containing polyol LDP-G3_{Cys}G3SF. The Cys-linker is shaded in purple. b) FQYs and normalized fluorescence intensities over time during the photobleaching study of fluorescein-conjugated LDPs-G3_{Cys}F and G3_{Cys}G3SF measured at the same conditions indicated in Figure 1.

imaging solution to prolong the lifetime of fluorophores under UV irradiation.³⁸⁻³⁹ However, the excessive amount of these agents that is required to achieve a protecting effect is usually enough to perturb cellular activities.⁴⁰⁻⁴²

Alternatively, anti-fading agents have been covalently conjugated to the dye itself,43 thereby eliminating the need of excessive amounts of these agents. Because thioether groups can be oxidized to sulfoxide and sulfone groups by reactive oxygen species (ROS), we took a similar approach and incorporated multiple thioether groups into the polymer backbone that might be sacrificially oxidized to protect the dye from bleaching. We designed a sulfide-rich ROMP monomer G3S and introduced multiple copies onto the LDP backbone (Figure 2a and Scheme S4, ESI†). Random ROMP copolymerization of monomers G3_{Cvs}, G3S, F and 3rd-generation Grubbs catalyst with a molar ratio of 20:5:2:1 resulted in water-soluble LDP-G3_{Cvs}G3SF (Figure 2a). Incorporating the G3S monomer led to a 16% improvement of the FQY compared to its non-thioether containing analogue, LDP-G3_{GIV}F (Figure 2b). Furthermore, sulfur-containing LDP-G3_{Cys}G3SF retained about 60% of its original fluorescence intensity after 4 h of irradiation, remaining twice as bright as irradiated LDP-G3_{GIV}F. These observations indicate that the multi-thioether-containing monomers provide an additional protective effect to improve the photostability of LDP- $\mathbf{G3}_{Gly}\mathbf{F}$ and may be applied to protect other fluorophores that are also sensitive to ROS.

Advanced PBI monomer

Because the FQY of PBI was not significantly improved with either the CDP or LDP scaffold (< 5%), we sought to use the modularity of the LDP platform to introduce an advanced PBI monomer. PBIs have attracted increasing attention because of their high thermal and photochemical stability, long emission wavelength, and high FQYs in organic solvents. 44-46 However, PBIs tend to aggregate in aqueous solution due to their polyaromatic cores resulting in fluorescence quenching. Charged groups have been introduced at the bay

Table 2. Photophysical properties of LDPs-G3_{Cys}PGx (x = 2, 3, or 4) at a concentration of 1.5 μ M for absorption and 0.15 μ M for emission measurements in 0.1 M PB at 20 °C.

LDP- G3 _{Cys} PGx	ϵ^a	\mathcal{O}_{f^b}	B^c
	(M ⁻¹ cm ⁻¹)	(%)	(M ⁻¹ cm ⁻¹)
LDP-G3 _{Cys} PG2	11 100	7.8	0.86
LDP-G3cysPG3	32 600	14	4.5
LDP-G3 _{cys} PG4	167 000	23	38

 $^{^{}o}$ Molar absorption coefficient ϵ , Equation S1, ESI[†]. b Fluorescence quantum yield \mathcal{O}_{f} , Equation S2, ESI[†]. c Brightness B, Equations S3, ESI[†].

regions of the PBI chromophore to provide water solubility and reduce aggregation.⁴⁷⁻⁴⁹ Despite their high FQYs, these charged PBI molecules inevitably arouse the concern of non-specific interactions when applied in cellular bioimaging.⁴⁴⁻⁴⁶ To address this concern, Zimmerman and coworkers studied bay-substituted PBIs with PG dendrons to afford neutral PBI fluorophores that maintain their high brightness and stability.⁵⁰ Haag and coworkers showed that imide-substituted dendronized PBIs have improved FQYs in water with increasing dendron generation.⁵¹⁻⁵³

Taking advantage of the intrinsically suppressed aggregation of dendronized PBIs, we introduced a PG dendron at the imideposition of the fluorophore to improve its FQY (see Scheme S6, ESI†). The PG dendron serves a two-fold purpose: the hydroxyl head groups increase the overall hydrophilicity of the molecule whereas the sterically-demanding structure minimizes fluorescence quenching via aggregation.50-56 The new dendronized PBI ROMPmonomer, PBIGx, features a PBI fluorophore core with an exonorbornenyl moiety on one end and a PG dendron in three different generations (G2, G3, or G4) at the other end (see Figure 3 and Scheme S6, ESI†). The exo-norbornenyl moiety allows the incorporation of PBI into the polymer backbone via a ROMP process. The molar absorption coefficients, FQYs, and brightness of the resulting LDPs-G3_{Cys}PGx improved with increasing dendron generation of the PBI monomer. The FQY of LDPs increased from 7.8% to 23% when the dendronized PBI monomer was changed from G2 to G4. (Table 2, also see Figure S10 b, ESI†). The increasing FQYs stem from the steric shielding effect of the dendrons, which can efficiently prevent intermolecular π - π stacking or dye-polymer self- quenching.50-53

FRET study

To further demonstrate the modularity of our LDPs, we incorporated two different fluorophores (C, F, B, PG4 and R) into the LDP platform to achieve new photophysical properties that are not available with individual fluorophores. The resulting bifluorophoric LDPs- $Gx_{Cys}Y_1Y_2$ (x=2 or 3) featured large Stokes shifts caused by FRET when the incorporated fluorophores had strong dipole-dipole interactions. Here we compared the FRET efficiency of various polymeric fluorophores with different backbones including linear CDP-precursors (pCDPs), globular CDPs, and short-chain LDPs with fluorescein and coumarin as the acceptor and donor groups, respectively (for structures of pCDPs and CDPs see Figure S6, ESI^{\dagger}).

The FRET efficiency was determined by the ratio of the acceptor and donor emission intensities ($I_{acceptor}$ / I_{donor} , Figure 3a, Figure S12, S13 and Table S4, ESI†), where the following rule applies: the higher the emission ratio, the higher the FRET efficiency. As shown in Figure 4b (left), a higher FRET efficiency was observed for CDPs than

Journal Name ARTICLE

for linear pCDPs with an NHS or tris function for crosslinking indicating that the CDPs are more compact in size than linear pCDPs. The FRET efficiency was improved by shortening the distance between the acceptor and donor fluorophores resulting from the crosslinking step. Short-chain LDPs provided a higher FRET efficiency than globular CDPs, suggesting that LDPs are more compact than CDPs and thus allow a closer proximity of the

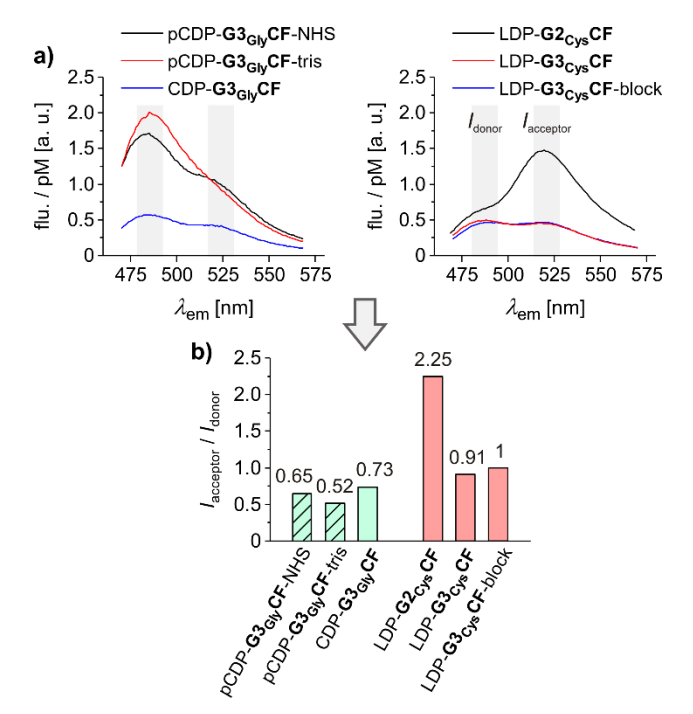


Figure 3. a) Fluorescence spectra and b) FRET efficiency of linear CDP precursors pCDPs, globular CDP, and short-chain LDPs with acceptor Fluorescein and donor Coumarin measured at 0.5 μ M in PB at 20 °C. The FRET efficiency was determined by the ratio of the maximum emission intensity ($I_{acceptor}$ / I_{donor}) of acceptor Fluorescein and donor Coumarin incorporated into different FRET polymers.

fluorophores. In the case of LDPs, random copolymerized LDP-G3_{Cys}CF and block copolymerized LDP-G3_{Cys}CF-block afforded comparable FRET, as shown in Figure 3b (right). In contrast, the FRET efficiency of LDP-G2_{Cys}CF increased significantly by using a lower molecular weight dendron monomer for polymerization. This observation suggests that the distance and flexibility between the two kinds of fluorophores was significantly influenced by the size of the incorporated dendron monomer. Presumably, the backbone of LDP-G2 is less crowded and more flexible than that of LDP-G3 or LDP-G3-block, which allowed for a higher FRET efficiency.⁵⁷⁻⁵⁸

The results above indicate that the FRET is more efficient in LDPs than in CDPs with the same dendron generation, showing that crosslinking of the polymer backbone is not necessary. In addition, FRET can be improved in LDPs by using a lower generation G2-dendron monomer. We envision that these new polymeric fluorophores with large Stokes shifts could eliminate spectral overlap between absorption and emission and allow for detection of fluorescence with reduced interference. 59-60 The fluorescence detection provided by this approach is particularly useful in quantitative molecular analysis where background effects need to be avoided for an efficient localization and quantification of the studied molecule. 61-62

Biological studies

In cell imaging studies, mounting media based on polyvinyl alcohol (PVA), e.g. Mowiol 4-88 or Gelvatol 20-30, are employed to improve the photostability of fluorophores. Although the stabilization mechanism is not fully understood, the polyol basis of these media seems to play a role in the photostabilization of the fluorophores. ⁶³⁻⁶⁴ Similar to these commercial PVAs, the LDPs provide multiple hydroxyl groups in close proximity to the fluorophores that may provide a similar stabilizing effect. To demonstrate the potential application of LDPs in biological studies, *in vitro* toxicity and uptake studies were performed on human epithelial HeLa cells. For these studies, G2- or G3-dendronized LDPs of Coumarin, Fluorescein, and PBIG4 were chosen due to their high brightness and different emission maxima.

A cytotoxicity study based on a sulforhodamine B (SRB) assay showed high cell viability at the tested concentration range between $10 - 100 \,\mu\text{g/mL}$, which indicates a good biocompatibility of

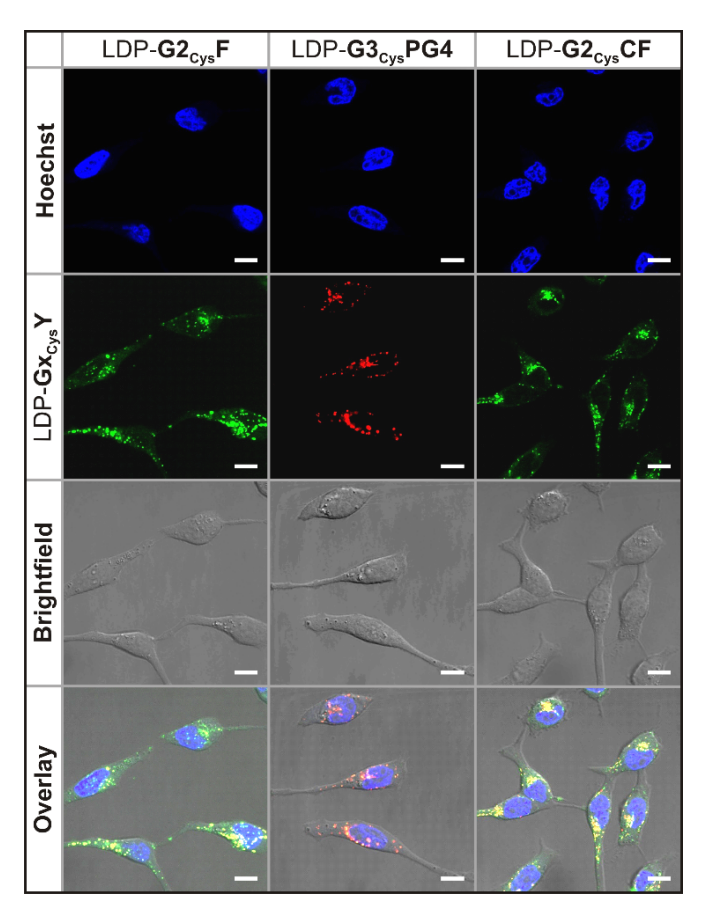


Figure 4. In vitro cellular uptake studies via live-cell microscopy of LDPs (7.5 μ g/mL) into HeLa cells after 4 h of incubation. First row: cell nuclei stained with Hoechst 33342 (blue). Second row: fluorescence from LDPs-Gxc_{vs}Y (x = 2 or 3) with Y = Coumarin (green), Fluorescein (green), and PBIG4 (red). Third row: brightfield. Fourth row: overlay of cell nuclei, fluorescence from LDPs, and brightfield. Scale bar: 10 μ m. LDPs (Figure S14, ESI†). The cellular uptake of LDPs was monitored by the live-cell confocal microscopy shown in Figure 4 (and Figure S15, ESI†). The entire series of dye-conjugated LDPs showed an intracellular signal after 4 h of incubation. The cells exhibit a vesicular staining pattern, presumably arising from cytoplasmic inclusions of the polymers into lysosomes and endosomes. In contrast, recently reported CDPs²⁶ showed a finely distributed uptake throughout the entire cytoplasm while ONPs²⁵ primarily localized in lysosomes. The low cytotoxicity and bright intracellular

ARTICLE Journal Name

signal renders these biocompatible dye-conjugated LDPs potential candidates for fluorescence bioimaging.

Conclusions

In summary, a broad series of fluorescent LDPs were synthesized in two steps on a modular basis and their photophysical properties characterized in an aqueous environment. The time-saving preparation for these new fluorescent polymeric nanoparticles eliminates the RCM step that requires a high loading of ruthenium catalyst. Furthermore, the streamlined synthesis for the new dendron monomer ${\bf G3}_{{\bf Cys}}$ reduces the synthetic effort by 7 steps compared to previously reported ${\bf G3}_{{\bf Gly}}$. Additionally, the optical properties of these LDPs can be fine-tuned by choosing different ratios and variants of dendron and fluorophore monomers.

The modular system provided by LDPs allowed the incorporation of different moieties, such as multi-sulfide-containing dendrons as anti-fading agents, dendronized fluorophores as intrinsic aggregation suppressors, or FRET pairs as potential improved imaging agents. LDPs showed high photostability, biocompatibility, and cellular uptake with bright intracellular fluorescence. Taken together, these results highlight new prospects for customized LDPs with any desirable ROMP-compatible fluorophore covering a broad spectrum of accessible wavelengths. The different staining patterns of ONPs, CDPs, and LDPs may be used for co-staining different cellular compartments for various applications. Furthermore, the decrease in Grubbs catalyst reduces the amount of toxic metals in the polymer preparation which renders LDPs a more environmentally friendly platform compared to ONPs or CDPs and thus makes them a better candidate for biological studies. Therefore, the reported LDPs represent a novel and versatile type of bright, stable, and biocompatible fluorophore.

Conflicts of interest

There are no conflicts to declare.

Acknowledgements

The authors acknowledge financial support of this project from the National Science Foundation NSF (CHE-1307404 and CHE-1709718) and from the Deutsche Forschungsgemeinschaft DFG (SFB 658).

Notes and references

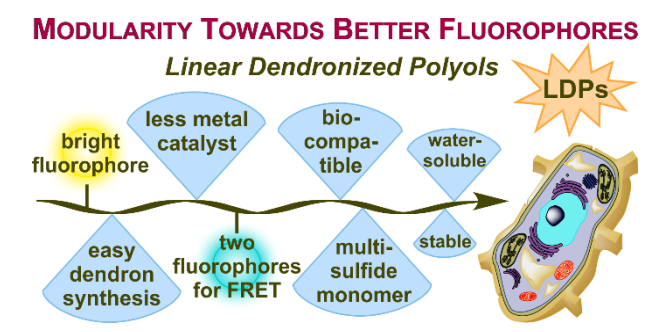
- B. N. G. Giepmans, S. R. Adams, M. H. Ellisman and R. Y. Tsien, Science, 2006, 312, 217-224.
- J. W. Lichtman and J.-A. Conchello, *Nat. Methods*, 2005, **2**, 910-919.
- 3 L. D. Lavis and R. T. Raines, *ACS Chem. Biol.*, 2008, **3**, 142-155.
- 4 M. Beija, C. A. M. Afonso and J. M. G. Martinho, *Chem. Soc. Rev.*, 2009, **38**, 2410-2433.
- 5 T. Ueno and T. Nagano, *Nat. Methods*, 2011, **8**, 642-645.
- 6 V. Sokolova and M. Epple, Nanoscale, 2011, 3, 1957-1962.
- 7 R. B. Altman, Q. Zheng, Z. Zhou, D. S. Terry, J. D. Warren and S. C. Blanchard, *Nat. Methods*, 2012, 9, 428-429.
- J. Chan, S. C. Dodani and C. J. Chang, Nat. Chem., 2012, 4, 973-984
- 9 K. P. Carter, A. M. Young and A. E. Palmer, Chem. Rev., 2014, 114, 4564-4601.

- 10 Z. Guo, S. Park, J. Yoon and I. Shin, Chem. Soc. Rev., 2014, 43, 16-29.
- 11 J. B. Grimm, T. A. Brown, A. N. Tkachuk and L. D. Lavis, *ACS Cent. Sci.*, 2017, **3**, 975-985.
- 12 P. Alivisatos, Nat. Biotechnol., 2004, 22, 47-52.
- 13 A. M. Smith, H. Duan, A. M. Mohs and S. Nie, *Adv. Drug Delivery Rev.*, 2008, **60**, 1226-1240.
- 14 C. Wu, B. Bull, C. Szymanski, K. Christensen and J. McNeill, ACS Nano, 2008, 2, 2415-2423.
- 15 J. Cheon and J.-H. Lee, Acc. Chem. Res., 2008, 41, 1630-1640.
- 16 D. Zheng, D. S. Seferos, D. A. Giljohann, P. C. Patel and C. A. Mirkin, *Nano Lett.*, 2009, 9, 3258-3261.
- 17 U. H. F. Bunz and V. M. Rotello, Angew. Chem., Int. Ed., 2010, 49, 3268-3279.
- R. A. Sperling and W. J. Parak, *Philos. Trans. R. Soc., A*, 2010, 368, 1333-1383.
- 19 J. A. Prescher and C. R. Bertozzi, *Nat. Chem. Biol.*, 2005, 1, 13-21.
- 20 Z. Liu, L. D. Lavis and E. Betzig, *Mol. Cell*, 2015, **58**, 644-659.
- 21 J. Hu, L. Dai and S. Liu, Macromolecules, 2011, 44, 4699-4710.
- 22 M. A. Sowers, J. R. McCombs, Y. Wang, J. T. Paletta, S. W. Morton, E. C. Dreaden, M. D. Boska, M. F. Ottaviani, P. T. Hammond, A. Rajca and J. A. Johnson, *Nat. Commun.*, 2014, 5, 5460.
- 23 M. P. Robin and R. K. O'Reilly, *Polym. Int.*, 2015, **64**, 174-182.
- 24 Z. M. Hudson, D. J. Lunn, M. A. Winnik and I. Manners, *Nat. Commun.*, 2014, 5, 3372.
- 25 Y. Bai, H. Xing, G. A. Vincil, J. Lee, E. J. Henderson, Y. Lu, N. G. Lemcoff and S. C. Zimmerman, *Chem. Sci.*, 2014, 5, 2862-2868.
- 26 Y. Li, Y. Bai, N. Zheng, Y. Liu, G. A. Vincil, B. J. Pedretti, J. Cheng and S. C. Zimmerman, *Chem. Commun.*, 2016, **52**, 3781-3784.
- 27 T.-L. Choi and R. H. Grubbs, Angew. Chem., Int. Ed., 2003, 42, 1743-1746
- 28 K. O. Kim and T.-L. Choi, ACS Macro Lett., 2012, 1, 445-448.
- 29 K. O. Kim and T.-L. Choi, *Macromolecules*, 2013, **46**, 5905-5914.
- 30 G.-J. Deng, B. Yi, Y.-Y. Huang, W.-J. Tang, Y.-M. He and Q.-H. Fan, *Adv. Synth. Catal.*, 2004, **346**, 1440-1444.
- 31 C. O. Liang, B. Helms, C. J. Hawker and J. M. J. Frechet, *Chem. Commun.*, 2003, DOI: 10.1039/B307425K, 2524-2525.
- 32 L. Sun, B. Zhu, Y. Su and C.-M. Dong, *Polym. Chem.*, 2014, 5, 1605-1613.
- 33 C.-M. Dong and G. Liu, Polym. Chem., 2013, 4, 46-52.
- 34 L. Song, E. J. Hennink, I. T. Young and H. J. Tanke, *Biophys. J.*, 1995, **68**, 2588-2600.
- 35 H. F. Blum and C. R. Spealman, *J. Phys. Chem.*, 1932, **37**, 1123-1133.
- 36 B. Hinkeldey, A. Schmitt and G. Jung, *ChemPhysChem*, 2008, 9, 2019-2027.
- 37 J. Mahmoudian, R. Hadavi, M. Jeddi-Tehrani, A. R. Mahmoudi, A. A. Bayat, E. Shaban, M. Vafakhah, M. Darzi, M. Tarahomi and R. Ghods, Cell J., 2011, 13, 169-172.
- 38 J. Vogelsang, R. Kasper, C. Steinhauer, B. Person, M. Heilemann, M. Sauer and P. Tinnefeld, Angew. Chem. Int. Ed., 2008, 47, 5465-5469.
- 39 I. Rasnik, S. A. McKinney and T. Ha, Nat. Methods, 2006, 3, 891-893
- 40 A. V. Mikhailov and G. G. Gundersen, *Cell Motil. Cytoskeleton*, 1995, **32**, 173-186.
- 41 A. Longin, C. Souchier, M. Ffrench and P. A. Bryon, *J. Histochem. Cytochem.*, 1993, **41**, 1833-1840.

Journal Name ARTICLE

- 42 Q. Zheng, M. F. Juette, S. Jockusch, M. R. Wasserman, Z. Zhou, R. B. Altman and S. C. Blanchard, *Chem. Soc. Rev.*, 2014, 43, 1044-1056.
- 43 R. B. Altman, D. S. Terry, Z. Zhou, Q. Zheng, P. Geggier, R. A. Kolster, Y. Zhao, J. A. Javitch, J. D. Warren and S. C. Blanchard, *Nat. Methods*, 2011, 9, 68.
- 44 D. Görl, X. Zhang and F. Würthner, Angew. Chem. Int. Ed., 2012, 51, 6328-6348.
- 45 T. Weil, T. Vosch, J. Hofkens, K. Peneva and K. Müllen, *Angew. Chem. Int. Ed.*, 2010, **49**, 9068-9093.
- 46 M. Sun, K. Müllen and M. Yin, Chem. Soc. Rev., 2016, 45, 1513-1528
- 47 K. Peneva, G. Mihov, F. Nolde, S. Rocha, J.-i. Hotta, K. Braeckmans, J. Hofkens, H. Uji-i, A. Herrmann and K. Müllen, *Angew. Chem. Int. Ed.*, 2008, **47**, 3372-3375.
- 48 M. A. Abdalla, J. Bayer, J. O. Raedler and K. Müllen, *Angew. Chem. Int. Ed.*, 2004, **43**, 3967-3970.
- 49 C. Kohl, T. Weil, J. Qu and K. Müllen, Chem. Eur. J., 2004, 10, 5297-5310.
- 50 S. K. Yang, X. Shi, S. Park, S. Doganay, T. Ha and S. C. Zimmerman, J. Am. Chem. Soc., 2011, 133, 9964-9967.
- 51 T. Heek, C. Kühne, H. Depner, K. Achazi, J. Dernedde and R. Haag, *Bioconjugate Chem.*, 2016, **27**, 727-736.
- 52 T. Heek, C. Fasting, C. Rest, X. Zhang, F. Würthner and R. Haag, *Chem. Commun.*, 2010, **46**, 1884-1886.
- 53 K. Huth, T. Heek, K. Achazi, C. Kühne, L. H. Urner, K. Pagel, J. Dernedde and R. Haag, *Chem. Eur. J.*, 2017, **23**, 4849-4862.
- 54 S. K. Yang, X. Shi, S. Park, T. Ha and S. C. Zimmerman, *Nat. Chem.*, 2013, **5**, 692-697.
- 55 A. T. Zill, K. Licha, R. Haag and S. C. Zimmerman, *New J. Chem.*, 2012, **36**, 419-427.
- 56 T. Heek, J. Nikolaus, R. Schwarzer, C. Fasting, P. Welker, K. Licha, A. Herrmann and R. Haag, *Bioconjugate Chem.*, 2013, 24, 153-158.
- 57 Y. Guo, J. D. van Beek, B. Zhang, M. Colussi, P. Walde, A. Zhang, M. Kröger, A. Halperin and A. Dieter Schlüter, J. Am. Chem. Soc., 2009, 131, 11841-11854.
- 58 O. Bertran, B. Zhang, A. D. Schlüter, M. Kröger and C. Alemán, J. Phys. Chem. C, 2015, 119, 3746-3753.
- 59 K. D. Piatkevich, J. Hulit, O. M. Subach, B. Wu, A. Abdulla, J. E. Segall and V. V. Verkhusha, *Proc. Natl. Acad. Sci. U.S.A.*, 2010, 107, 5369-5374.
- 60 T. Kogure, S. Karasawa, T. Araki, K. Saito, M. Kinjo and A. Miyawaki, *Nat. Biotechnol.*, 2006, **24**, 577-581.
- 61 D. M. Shcherbakova, M. A. Hink, L. Joosen, T. W. J. Gadella and V. V. Verkhusha, J. Am. Chem. Soc., 2012, 134, 7913-7923.
- 62 P. Hou, S. Chen, H. Wang, J. Wang, K. Voitchovsky and X. Song, *Chem. Commun.*, 2014, **50**, 320-322.
- 63 M. Ono, T. Murakami, A. Kudo, M. Isshiki, H. Sawada and A. Segawa, *J. Histochem. Cytochem.*, 2001, **49**, 305-311.
- 64 A. Longin, C. Souchier, M. Ffrench and P. Bryon, *J. Histochem. Cytochem.*, 1993, **41**, 1833-1840.

Table of Contents (TOC)



Linear dendronized polyols (LDPs) as a modular platform for bright, stable, and biocompatible polymeric fluorophores applicable for fluorescent bioimaging studies.